Analyst

Accepted Manuscript

ROYAL SOCIETY OF CHEMISTRY

www.rsc.org/analyst

Label-Free Fluorescence Polarization Detection of Pyrophosphate Based on 0D/1D Fast Transformation of CdTe Nanostructures

Jinyan Du, Li Ye, Meili Ding, Yuting Chen, Shujuan Zhuo, Changqing Zhu*

Key Laboratory of Functional Molecular Solids, Ministry of Education; Anhui Key Laboratory of Chemo-Biosensing, College of Chemistry and Materials Science, Anhui Normal University, Wuhu, 241000, PR China

Abstract: A novel and label-free fluorescence polarization (FP) method for the determination of pyrophosphate (PPi) was developed based on the change in FP signals during fast reversible transformation between CdTe zero-dimensional (0D) nanocrystals (NCs) and one-dimensional (1D) nanorods (NRs) as induced by addition of PPi. Under optimum conditions, the FP ratio was linearly proportional to the logarithm of the concentration of PPi between 2.0×10^{-5} and 1.0×10^{-9} M with a detection limit of 8.0×10^{-10} M. The developed method, with high signal selectivity and stability, was successfully applied to the detection of PPi in human urine samples.

Keywords: fluorescence polarization, CdTe nanocrystals, fast transformation, PPi, human urine sample

1. Introduction

* Corresponding author.
E-mail address: zhucq@mail.ahnu.edu.cn

Anions play important roles in the fields of biological, chemical, and environmental processes.[1-4] Pyrophosphate (PPi) is proved as an essential anion for normal cellular functioning and has numerous applications in biology.[5-8] Naturally, the selective detection of PPi becomes a major research focus. So far, the detection methods of PPi such as fluorescence chemosensing,[9-18] colorimetric,[19-22] enzyme,[23, 24] electrogenerated chemiluminescence (ECL)[25] and chromatographic method[26] were developed. Among which, fluorescence chemosensing method based on the change of fluorescence intensity signals, has been received intensive attention.[12] In order to improve the selectivity of signals, ratiometric fluorescence (eliminating the instability of fluorescence intensity signals),[10] infrared or near-infrared emission (avoiding the disturbance in short wavelength),[27] and time-resolved fluorescence (deleting the noise from short lifetime substances),[28] etc, have been applied. In fact, fluorescence polarization (FP) signals also have good selectivity.[29] However, the detection method of PPi based on FP signals has not been reported up to now. The reason is that obtaining measurable degree of polarization values is difficult because the rate of rotational diffusion is typically faster than the rate of emission for small fluorophores in low-viscosity solutions. Under these conditions, emissions are depolarized.[30] To acquire measurable FP signal changes, the fluorescent probe must first be labeled with macromolecules, after which the rotational diffusion rate of the whole molecule is changed through analyte-induced or molecular interactions.[31] Similar to the use of fluorescence intensity signal, however, whether or not it is possible to build fluorescence sensing system based on FP signal changes without labeling.

Fortunately, many recent important discoveries about zero-dimensional (0D) light-emitting quantum dots (QDs), one-dimensional (1D) and two-dimensional (2D) materials have brought about opportunities for the development of novel fluorescence sensing system. Whereas some 1D nanorods (NRs) show a large extent of polarization, 0D nanoparticles (NPs) show much smaller extents of polarization[32,33]. According to previous literatures[34,35,36,37], 0D NPs can be transformed to 1D NRs or nanowires (NWs). Recently, we discovered and studied a system featuring fast reversible transformation between CdTe 0D NCs and 1D NRs triggered by ions.[38] Herein, we construct a simple, feasible, and label-free assay for detecting PPi by taking advantage of significant changes in FP signals that occur during the above transformation process. Interference tests showed that FP signals are more reliable than fluorescence intensity and lifetime signals. The proposed method was applied in the detection of PPi in dilute urine samples, and the recovery was found to be in the range of 95.2% to 103%. Our developed method presents a novel label-free approach for directly detecting small molecules like PPi.

2. Experiment

2.1 Reagents

Te powder (~60 mesh, 99.999%), thioglycolic acid (TGA, 99%), L-cysteine hydrochloride monohydrate (L-cys, 98%) and europium nitrate hexahydrate [$Eu(NO_3)_3 \cdot 6H_2O$, abbreviated Eu(III), 99.99%] were purchased from Alfa Aesar (Karlsruhe, Germany). Cadmium chloride hemi (pentahydrate) ($CdCl_2 \cdot 2.5H_2O$),

$NaBH_4$, sodium pyrophosphate ($Na_4P_2O_7$, abbreviated PPi), and other routine chemicals were acquired from Guoyao Chemical Reagent Company (Shanghai, China) and used as received without further purification. All chemicals used were of analytical grade or the highest purity available. All solutions were prepared with double deionized water (DDW). All experiments described hereafter were performed under ambient conditions.

2.2 Apparatus

All steady-state fluorescence measurements were made with a Hitachi F-4500 fluorescence spectrophotometer (Tokyo, Japan) equipped with a R3896 red-sensitive multiplier and a 1 cm quartz cell. Ultraviolet−visible (UV−vis) absorption spectra were recorded with a Hitachi U-3010 spectrophotometer (Tokyo, Japan). Transmission electron microscopy (TEM) images were acquired using a JEOL JEM-2010 instrument operating at an acceleration voltage of 200 kV. Dilute solutions of the CdTe NCs and NRs were deposited onto copper grids with a carbon support by slowly evaporating the solvent in air at room temperature. Fluorescence anisotropy lifetime and FP signals were measured via the time-correlated single-photo counting technique on a combined steady-state and lifetime spectrometer (Edinburgh Analytical Instruments, FLS920). All pH values were measured with a model PHS-3C meter (Hangzhou, China).

2.3 Fluorescence Measurements and Parameter Determination

In a typical test, 760 μL of the CdTe NC solution and certain amounts of Eu(III) were sequentially added into a calibrated test tube, and then PPi was added to this

solution. The mixture was diluted to 2 mL with DDW and mixed thoroughly for 30 min. Finally, the fluorescence intensity, anisotropy lifetime and polarization of CdTe nanostructures were measured at room temperature (25 ± 1 °C). Fluorescence detection of different samples was performed under the same conditions: the excitation wavelength was set to 380 nm and the slit widths of excitation and emission were both 5 nm. The fluorescence intensity was recorded in the wavelength range of 420 - 700 nm. During FP measurement of the CdTe nanostructures, polyacrylamide (PAM, 5.0% in concentration) was added to the samples to terminate reaction process and stabilize the signals. The emission wavelength was set to the fluorescence emission peak position with excitation at 380 nm. The intensity of emission was measured through a polarizer. When the emission polarizer is oriented parallel (||) to the direction of the polarized excitation, the observed intensity is called $I_{\parallel}$. Likewise, when the polarizer is oriented perpendicular ($\perp$) to the excitation, the intensity is called $I_{\perp}$. These intensity values were used to calculate the fluorescence anisotropy.

$$r = \frac{I_{\parallel} - I_{\perp}}{I_{\parallel} + 2I_{\perp}}$$

The polarization is given by

$$P = \frac{I_{\parallel} - I_{\perp}}{I_{\parallel} + I_{\perp}}$$

The polarization and anisotropy values can be interchanged using

$$P = \frac{3r}{2 + r}$$

The anisotropy decay, r(t) , was deduced according to the equation below[30]

$$r(t) = \frac{I_{VV}(t) - G \cdot I_{VH}(t)}{I_{VV}(t) + 2G \cdot I_{VH}(t)}$$

in which the G factor was calculated by $G = I_{HV}(t) / I_{HH}(t)$, I represents the intensity of the fluorescence signal and the subscripts denotes the orientation of the excitation and emission polarizers (H for horizontal and V for vertical), respectively. In the exponential fitting of the anisotropy decay signal, the time when the signal of the prompt reaches its maximum is treated as the time zero point because the prompt signal reflects the instrumental response.

3. Results and Discussion

3.1 Reversible Transformation of 0D/1D CdTe Nanostructures

CdTe NCs were synthesized and pretreated based on the reported approach[39,38]. The treated NCs were redissolved in NaOH solution (pH 11.00) for further studies. According to the formula proposed by Yu et al. [40], the concentration of the CdTe NC solution is determined as 1.90×10^{-5} M. Fig. 1A shows the TEM images of the CdTe NCs with an emission peak of 520 nm (Fig. 2A, curve a). The average size of the particles is approximately 4 nm. Surprisingly, 30 min after addition of Eu(III) to the treated CdTe NCs, CdTe NRs with average width of ca. 15 nm were observed (Fig. 1B). The fluorescence maximum and UV-vis absorption spectrum show a bathochromic shift (Fig. 2, curve b), which indicates an increase in the overall size of the NPs[37]. The FP signals increase significantly (Fig. S1). In our previous work[38], these experiment facts have been reported, and a detailed explanation has been presented.

It's worth mentioning that as-induced 1D NRs were disaggregated into 0D NCs

within 30 min after addition of low concentrations of PPi (Fig. 1C), and the fluorescence maximum basically shift toward the emission wavelength of NCs (Fig. 2A, curve c) with rough recovery of UV-vis absorption spectrum. It is surprising that the FP signals decrease significantly under this condition (Fig. S1). However, directly synthesized NRs are not disaggregated by PPi (Fig. S2). XPS results show that the as-induced NRs contain element of Eu, about 0.94% (wt%)[38]. To evaluate the binding affinities of Eu(III)/CdTe, Eu(III)/PPi and CdTe/PPi, the effect of various concentration of PPi on the quenched fluorescent intensity of CdTe NCs triggered by Eu(III) was investigated. The fluorescence quenching can be described by the Stern-Volmer equation.[41] Fig. S3 A, B and C show the Eu(III) concentration-dependent quenching of the fluorescence intensity of the CdTe NCs in the presence of different PPi concentration, and Fig. S3 D gives the Stern-Volmer plots for Eu(III). Weaker fluorescence quenching can be observed at higher PPi concentration in the presence of the same Eu(III) concentration (Fig. S3 D). With increasing of the PPi concentration, fluorescence intensity is gradually enhanced (Fig. S3 E). The protective effect of PPi toward CdTe NCs is understandable because of the strong coordination between PPi and Eu(III), in which the stability constant (K) of the complex formed by Eu(III) and PPi is higher than that of the complex formed by Eu(III) and carboxyl (or cysteine).[42, 43] Therefore, we suggest that the competitive coordination of Eu(III) with CdTe surface-confined carboxyl (cysteine) and PPi is responsible for 0D/1D transformation of CdTe nanostructures and the corresponding FP signal changes (Scheme 1).

In order to further investigate CdTe/Eu(III)/PPi complex behaviors in solution, time-resolved fluorescence anisotropy decays of CdTe/Eu(III)/PPi complex were examined in 5% PAM water solution. The fluorescence anisotropy decays for CdTe, CdTe/Eu and CdTe/Eu/PPi during the first 14 ns after excitation are presented in Fig. 3. All curves in Fig. 3 are fitted with exponential function and the derived parameters of anisotropy lifetimes (τ), rotational correlation times (θ) and limiting anisotropy (r_0) are summarized in Table S1. Three well-defined rotational motions were found, namely, the fast motions of CdTe NCs with smaller θ of 0.261 ns, the slow motions of CdTe/Eu complex with θ of 0.557 ns and the fast motions of CdTe/Eu/PPi complex with θ of 0.360 ns. Obviously, the remarkable variation of θ is caused by the shape and size change of CdTe nanostructures,[30] which is in accordance with the variation of r_0 (Table S1). This results imply that the aggregation of CdTe NCs induced by Eu(III) ions is restricted by PPi molecules. Considering these findings, we believe that the disaggregation effect of PPi is probably related to the strong coordination preference between Eu(III) and PPi, which causes the as-induced CdTe NRs to collapse. Importantly, the observed decrease in FP signals provides appropriate preconditions for sensing PPi during the transformation process of CdTe NRs to NCs.

3.2 Probe Optimization

3.2.1 Optimization of the Concentration of CdTe NCs

To investigate the effect of the concentration of the CdTe NCs, a series of calibration functions, the FP against the concentration of Eu(III) ions, were obtained with various concentrations of the CdTe NCs. Fig. 4 shows FP changes increase

slowly with increasing concentration of CdTe NCs, and begin to decline at a concentration of 7.2×10^{-6} M. According to the literature[44], excessive concentrations of NCs are disadvantageous to their preferential growth along a certain axis. When the concentration of NCs is extremely low, the FP signal of as-induced NRs weakened, resulting in narrowing linear range of the calibration function. The optimal concentration of the NCs may be expected to give the maximum sensitivity (i.e. the slope of calibration function) and the widest linear range of the calibration function. To balance the sensitivity and linear range of the calibration function, a 7.2×10^{-6} M of the CdTe NC solution is employed for further experiments.

3.2.2 Optimization of Eu(III) Ions Concentration

The effect of concentration of Eu(III) ions on the FP signals was investigated and the results are shown in Fig. 5. The FP signal increases with increasing concentration of Eu(III) ions, and reaches maximum at a concentration of 1.45×10^{-7} M. With further increasing in concentration, however, the FP signal significantly decreases. Differences in the aspect ratio of the as-induced CdTe NRs at different concentrations of Eu(III) ions could account for the FP change observed[45]. Appropriate reduction of the Eu(III) ion concentration facilitates analytical sensitivity. However, when the concentration of Eu(III) ion is excessively low, the linear range narrows considerably. Thus, in this work, a 1.2×10^{-7} M Eu(III) ion solution is used for further experiments.

3.2.3 Optimization of pH

CdTe NCs are unstable under acidic conditions[46], and precipitation of $Eu(OH)_3$ [K_{sp} of $Eu(OH)_3$ $=8.9 \times 10^{-24}$] occurs in strongly alkaline conditions. Based on our

calculations, when the concentration of Eu(III) ion is 1.2×10^{-7} M, $Eu(OH)_3$ is formed at pH 8.62. Thus, the effects of pH between 7.00 and 9.50 on the FP signals were studied to determine optimum conditions for the detection of PPi. From Fig. 6, the maximum change value of the FP of the CdTe nanostructures is obtained at pH 8.10. Thus, 0.1 M Tris-HCl buffer solutions (pH 8.10) are used for further experiments.

3.2.4 Optimization of the Reaction Time

The effect of time on the FP signals of the system was tested. Experiments show that FP signals reach maxima when the CdTe NC solution is incubated with Eu(III) ions at room temperature for 30 min (Fig. S4). PPi is added subsequently to the above system after maximum FP signals with Eu(III) ions are achieved, and the FP signals are recorded at intervals of a couple of minutes (Fig. S5). The result show that FP signals reach a minimum after 10 min, and then PAM is added to the system, meanwhile, the FP signals are recorded continuously (Fig. S6). It was shown that the FP signals keep stable for over 120 min, long enough to record the FP signals of the system with PPi.

3.2.5 Tolerance and Selectivity Test

To assess the selectivity of the proposed method, tolerance levels for coexisting foreign substances were tested. Tables 1 and 2 show the results of the interference tests. Most of the tested common ions can be presented at relatively high concentrations through FP signals. Some cations with strong coordination ability, such as Ca(II) and Cd(II) ions[47], are tolerated at relatively low levels, probably because these cations are also involved in the transformation of CdTe NCs to NRs. Moreover,

high concentrations of common complexants (eg. EDTA) interfere with the detection of PPi to some extent. However, due to difference of coordination ability, the FP signals are scarcely influenced by PO_4^{3+} (Pi), in agreement with our proposed mechanism of disaggregation of as-induced NRs by PPi. Tables 1 and 2 indicate that interfering ions affect the fluorescence intensity and lifetime signals to a great extent, while the FP signals are hardly affected. These findings demonstrate the reliability of FP signals.

3.2.6 Analytical Performance

The FP signals of Eu(III)-induced CdTe NRs with PPi were recorded at optimal experimental conditions. The FP signals of as-induced CdTe NRs significantly decreased with increasing PPi concentration. A good linear relationship (R=0.995) is found between the FP ratios and the logarithm of the concentration of PPi over the range from 2.0×10^{-5} M to 1.0×10^{-9} M (Fig. 7); the limit of detection (LOD), calculated following the 3σ IUPAC criteria[48], is 8.0×10^{-10} M. The relative standard deviation for six replicate measurements of a solution containing 2.0×10^{-7} M PPi is 1.9%. Therefore, the present method is both highly sensitive and reproducible. The calibration equation obtained in our experiments was

$$\frac{P_0 - P}{P_0} = 1.36 + 0.108 \log c$$

Where P_0 and P are the FP signals of as-induced NRs in the absence and presence of PPi, respectively, and c is the concentration of PPi.

The proposed method was applied in the determination of PPi in urine sample. The samples were processed as described in the literature[10], then diluted 1.8-fold as

experimental samples, and the results are given in Table 3. The results are in good agreement with a previous report[10] and the recovery is 95.2-103%. On comparison with the results in the literatures (Table S2), our method has broader linear range and lower limit of detection. These findings suggest that the present method is both reliable and practical.

4. Conclusion

In summary, a novel and label-free FP method for detecting PPi was constructed based on the change in FP signals during rapid transformation from as-induced CdTe 1D NRs to 0D NCs as triggered by the analyte. Compared with other fluorescence signals, FP signals were found to be hardly interfered, indicative of high reliability. Our developed method was successfully applied in the detection of PPi in dilute urine samples with recovery of 95.2% - 103%. Thus, our method presents a new approach for directly detecting small molecules like PPi.

Acknowledgements

This work was financially supported by the National Natural Science Foundation of China (No. 21175003 and 21375003).

References

1. M. Weller, *Protein phosphorylation*, Pion Ltd., 1979.
2. P. Chakrabarti, *J. Mol. Biol.*, 1993, **234**, 463-482.
3. P. Bodin and G. Burnstock, *Neurochem. Res.*, 2001, **26**, 959-969.
4. J. M. Berg, *Acc. Chem. Res.*, 1995, **28**, 14-19.
5. D. C. SiLcox and D. J. McCarty, *Journal of Clinical Investigation*, 1973, **52**, 1863.
6. M. Ronaghi, S. Karamohamed, B. Pettersson, M. Uhlén and P. Nyrén, *Anal. Biochem.*, 1996, **242**, 84-89.

7. G. V. Zyryanov, M. A. Palacios and P. Anzenbacher, *Angew. Chem. Int. Ed.*, 2007, **46**, 7849-7852.
8. P. D. Beer and P. A. Gale, *Angew. Chem. Int. Ed.*, 2001, **40**, 486-516.
9. Y. Liu and K. S. Schanze, *Anal. Chem.*, 2008, **80**, 8605-8612.
10. N. Shao, H. Wang, X. Gao, R. Yang and W. Chan, *Anal. Chem.*, 2010, **82**, 4628-4636.
11. P. Das, N. B. Chandar, S. Chourey, H. Agarwalla, B. Ganguly and A. Das, *Inorg. Chem.*, 2013, **52**, 11034-11041.
12. Y. Mikata, A. Ugai, R. Ohnishi and H. Konno, *Inorg. Chem.*, 2013, **52**, 10223-10225.
13. S. Nishizawa, Y. Kato and N. Teramae, *J. Am. Chem. Soc.*, 1999, **121**, 9463-9464.
14. Y. Bao, H. Wang, Q. Li, B. Liu, Q. Li, W. Bai, B. Jin and R. Bai, *Macromolecules*, 2012, **45**, 3394-3401.
15. Z. Guo, W. Zhu and H. Tian, *Macromolecules*, 2010, **43**, 739-744.
16. T. Gunnlaugsson, A. P. Davis, J. E. O'Brien and M. Glynn, *Org. Lett.*, 2002, **4**, 2449-2452.
17. L. J. Liang, X. J. Zhao and C. Z. Huang, *Analyst*, 2012, **137**, 953-958.
18. R. Villamil-Ramos, V. Barba and A. K. Yatsimirsky, *Analyst*, 2012, **137**, 5229-5236.
19. J. Deng, P. Yu, L. Yang and L. Mao, *Anal. Chem.*, 2013, **85**, 2516-2522.
20. D. H. Lee, J. H. Im, S. U. Son, Y. K. Chung and J.-I. Hong, *J. Am. Chem. Soc.*, 2003, **125**, 7752-7753.
21. S. Bhowmik, B. N. Ghosh, V. Marjomäki and K. T. Rissanen, *J. Am. Chem. Soc.*, 2014, DOI: 10.1021/ja4128949.
22. C. R. Lohani, J.-M. Kim, S.-Y. Chung, J. Yoon and K.-H. Lee, *Analyst*, 2010, **135**, 2079-2084.
23. B. K. Datta, S. Mukherjee, C. Kar, A. Ramesh and G. Das, *Anal. Chem.*, 2013, **85**, 8369-8375.
24. R. K. Pathak, V. K. Hinge, A. Rai, D. Panda and C. P. Rao, *Inorg. Chem.*, 2012, **51**, 4994-5005.
25. I.-S. Shin, S. W. Bae, H. Kim and J.-I. Hong, *Anal. Chem.*, 2010, **82**, 8259-8265.
26. S. M. Marques, F. Peralta and J. C. Esteves da Silva, *Talanta*, 2009, **77**, 1497-1503.
27. T. Cheng, T. Wang, W. Zhu, X. Chen, Y. Yang, Y. Xu and X. Qian, *Org. Lett.*, 2011, **13**, 3656-3659.
28. D. Zhu, Y. Chen, L. Jiang, J. Geng, J. Zhang and J.-J. Zhu, *Anal. Chem.*, 2011, **83**, 9076-9081.
29. D. Zhang, H. Shen, G. Li, B. Zhao, A. Yu, Q. Zhao and H. Wang, *Anal. Chem.*, 2012, **84**, 8088-8094.
30. J. R. Lakowicz, *Principles of fluorescence spectroscopy*, Springer, 2009.
31. J. Ruta, S. Perrier, C. Ravelet, J. Fize and E. Peyrin, *Anal. Chem.*, 2009, **81**, 7468-7473.
32. S. Acharya, D. Sarma, Y. Golan, S. Sengupta and K. Ariga, *J. Am. Chem. Soc.*, 2009, **131**, 11282-11283.
33. J. Giblin, V. Protasenko and M. Kuno, *ACS nano*, 2009, **3**, 1979-1987.
34. Z. Tang, N. A. Kotov and M. Giersig, *Science*, 2002, **297**, 237-240.
35. H. Zhang, D. Wang, B. Yang and H. Möhwald, *J. Am. Chem. Soc.*, 2006, **128**, 10171-10180.
36. Y. Volkov, S. Mitchell, N. Gaponik, Y. P. Rakovich, J. F. Donegan, D. Kelleher and A. L. Rogach, *ChemPhysChem*, 2004, **5**, 1600-1602.
37. P. V. Nair and K. G. Thomas, *The Journal of Physical Chemistry Letters*, 2010, **1**, 2094-2098.
38. J. Du, X. Dong, S. Zhuo, W. Shen, L. Sun and C. Zhu, *Talanta*, 2014, **122**, 229-233.
39. J. Li, X. Hong, D. Li, K. Zhao, L. Wang, H. Wang, Z. Du, J. Li, Y. Bai and T. Li, *Chem.*

Commun., 2004, 1740-1741.

40. W. W. Yu, L. Qu, W. Guo and X. Peng, *Chem. Mater.*, 2003, **15**, 2854-2860.
41. P. Wu, Y. Li and X.-P. Yan, *Anal. Chem.*, 2009, **81**, 6252-6257.
42. R. Jonasson, G. Bancroft and H. Nesbitt, *Geochim. Cosmochim. Acta*, 1985, **49**, 2133-2139.
43. R. H. Byrne, X. Liu and J. Schijf, *Geochim. Cosmochim. Acta*, 1996, **60**, 3341-3346.
44. X. Peng, L. Manna, W. Yang, J. Wickham, E. Scher, A. Kadavanich and A. P. Alivisatos, *Nature*, 2000, **404**, 59-61.
45. J. Hu, L.-s. Li, W. Yang, L. Manna, L.-w. Wang and A. P. Alivisatos, *Science*, 2001, **292**, 2060-2063.
46. V. Swayambunathan, D. Hayes, K. H. Schmidt, Y. Liao and D. Meisel, *J. Am. Chem. Soc.*, 1990, **112**, 3831-3837.
47. S. Mayilo, J. Hilhorst, A. S. Susha, C. Höhl, T. Franzl, T. A. Klar, A. L. Rogach and J. Feldmann, *J. Phys. Chem. C*, 2008, **112**, 14589-14594.
48. A. M. Committee, *Analyst*, 1987, **112**, 199-204.

Scheme 1 Kinetic scheme of the Eu(III)/CdTe/PPi complex formation.

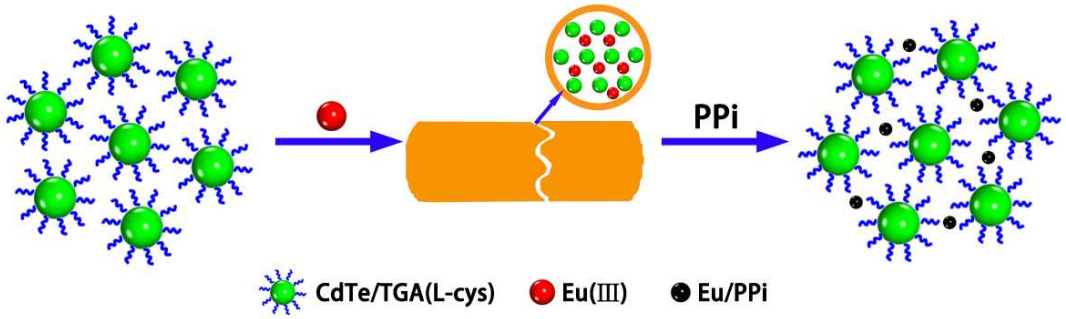

Figure Captions

Fig. 1 (A) TEM image of CdTe NCs; (B) TEM image of CdTe NRs 30 min after addition of 1.0×10^{-7} M Eu(III) ions; (C) TEM image of (B) 30 min after addition of 2.0×10^{-7} M PPi.

Fig. 2 (A) Fluorescence spectra of (a) CdTe NCs (magenta circle); (b) as-induced CdTe NRs 30 min after addition of 1.0×10^{-7} M Eu(III) ions (green triangle); (c) as-disaggregated NCs 30 min after addition of 2.0×10^{-7} M PPi (blue square); (B) Absorption spectra of (a) CdTe NCs (magenta circle); (b) as-induced CdTe NRs 30 min after addition of 1.0×10^{-7} M Eu(III) ions (green triangle); (c) as-disaggregated NCs 30 min after addition of 2.0×10^{-7} M PPi (blue square).

Fig. 3 Time-resolved fluorescence anisotropy decays of CdTe NCs (green square); CdTe NCs after addition of 1.0×10^{-7} M Eu(III) ions (red circle); as-induced CdTe NRs after addition of 2.0×10^{-7} M PPi (blue triangle).

Fig. 4 Effect of CdTe NCs concentration on the relative FP signals in the absence (P_0) and presence (P) of Eu(III) ion. The concentration of Eu(III) ions is 1.0×10^{-7} M.

Fig. 5 FP signals of the CdTe NCs upon addition of Eu(III) ions (0, 2.0, 5.0, 7.0, 10.0, 15.0, 17.0, 18.0, 19.0, 22.0, 25.0 and 27.0×10^{-7} M). Results show mean ± standard deviation in six assays.

Fig. 6 Effect of pH on the relative FP signals of as-induced NRs before (P_0) and after (P) addition of PPi. The concentration of Eu(III) ions and PPi is 1.2×10^{-7} M and 2.0×10^{-7} M, respectively.

Results show mean ± standard deviation in six assays.

Fig. 7 Plot of FP ratios $[(P_0-P)/P_0]$ of as-induced CdTe NRs at peak emission versus the logarithm of the concentration of PPi. Results show mean ± standard deviation in six assays.

Fig. 1

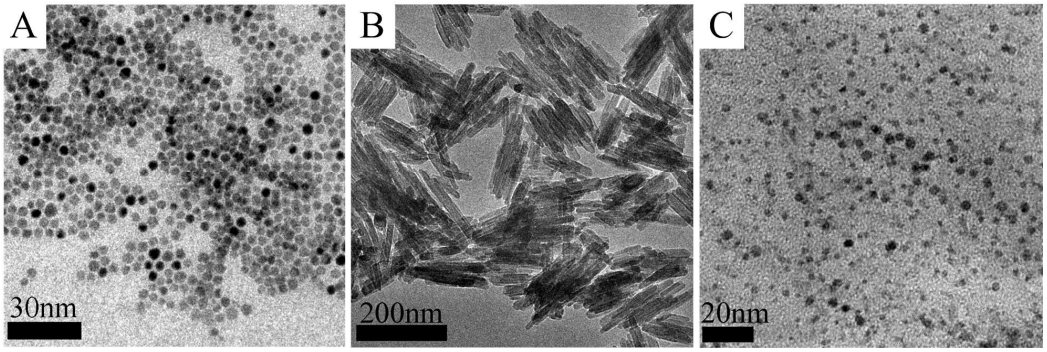

Fig. 2

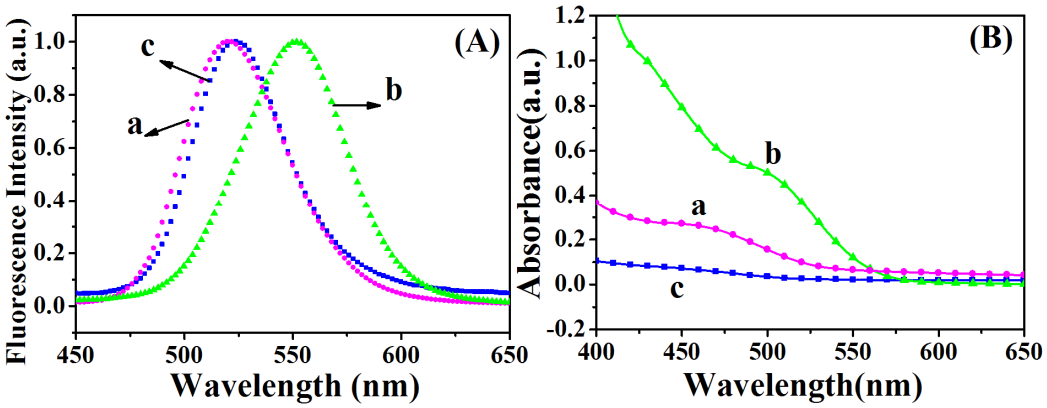

Fig. 3

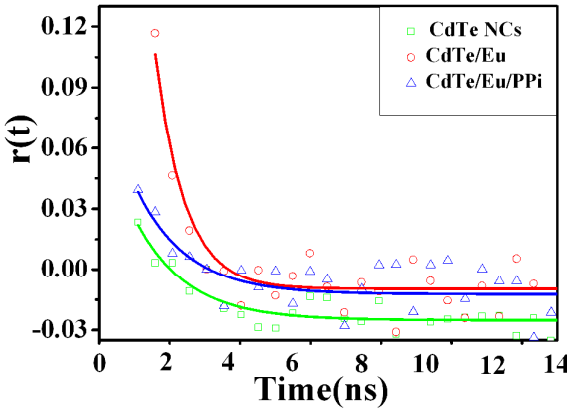

Fig. 4

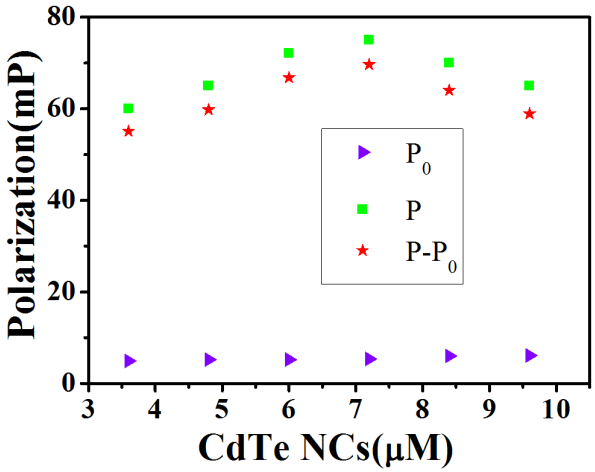

Fig. 5

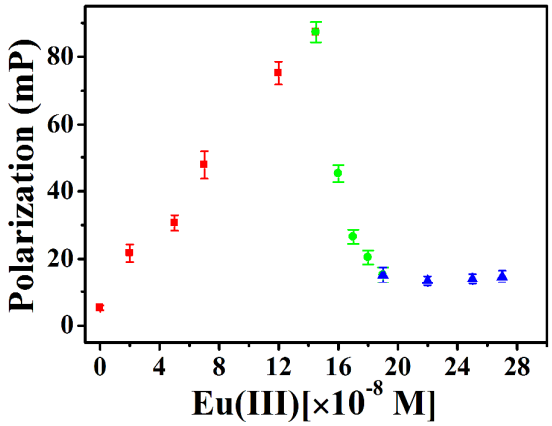

Fig. 6

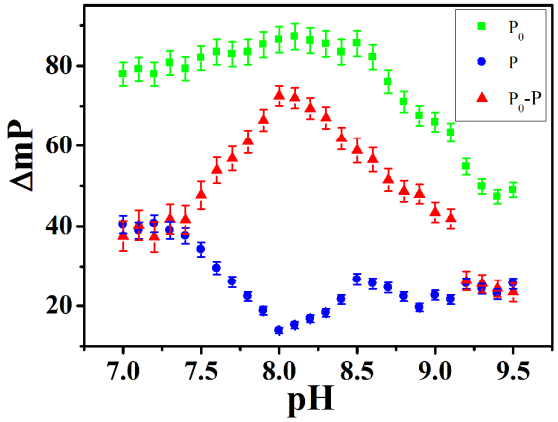

Fig. 7

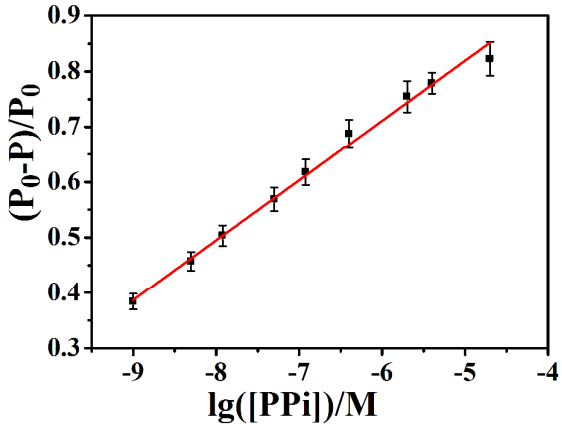

Table Captions

Table1. Interferences from some coexisting cations

Table2. Interferences from some coexisting anions

Table 3 Determination of PPi in real samples

Table 1

Coexisting substance	*Coexisting concentration ($\times 10^{-7}$ mol·L^{-1})*	*Change of fluorescence intensity (%)*	*Change of fluorescence life-time (%)*	*Change of fluorescence polarization (%)*
Non	-	0	0	0
Ba^{2+}	100	-23.2	1.4	2.3
Mg^{2+}	100	-19.3	-3.2	4.4
Fe^{2+}	100	2.4	2.2	-2.5
Cu^{2+}	100	10.8	75.8	4.5
Ca^{2+}	10	-3.1	3.6	2.3
Zn^{2+}	100	5.5	4.3	-1.9
Ag^{+}	100	32.9	58.3	2.5
Pb^{2+}	100	-2.6	6.9	-1.7
Hg^{2+}	100	-76.1	33.6	7.5
Cd^{2+}	10	-3.9	8.0	4.1
Mn^{2+}	100	-14.8	22.9	0.96
Co^{2+}	100	-3.6	34.9	-0.60
Cr^{3+}	100	-16.1	21.4	1.1

The concentration of CdTe NCs is 7.2×10^{-6} M and the concentration of Eu(III) ions is 1.2×10^{-7} M.

The coexisting anion is Cl^-.

Table 2

Coexisting substance	*Coexisting concentration ($\times 10^{-7}$ mol·L^{-1})*	*Change of fluorescence intensity (%)*	*Change of fluorescence life-time (%)*	*Change of fluorescence polarization (%)*
Non	-	0	0	0
F^-	150	-13.0	1.7	0.8
$B_4O_7^{2-}$	150	-56.6	15.0	2.2
NO_2^-	150	12.8	8.8	3.1
$S_2O_3^{2-}$	150	-10.3	21.6	1.9
EDTA	150	-16.2	22.5	-15.9
SO_3^{2-}	150	12.4	1.3	0.2
I^-	150	12.2	-2.2	-1.1
SO_4^{2-}	150	39.1	-10.3	-3.6
NO_3^-	150	24.7	-4.5	1.1
S^{2-}	150	-54.1	-4.4	-2.2
SCN^-	150	-3.1	22.8	-0.9
dopamine	150	11.2	20.1	3.2
$(NH_4)_2Mo_4O_{13}$	150	-48.9	-29.9	-3.4
$C_9H_{11}NO_2$	150	-3.4	9.9	-1.5
PO_4^{3-}	150	-8.6	5.2	-2.3

The concentration of CdTe NCs is 7.2×10^{-6} M, the concentration of Eu(III) ions is 1.2×10^{-7} M, and the concentration of PPi is 2.0×10^{-7} M. The coexisting cation is Na^+.

Table 3

Samples	*PPi founded/10^{-6} M* [a,b]	*PPi added/10^{-6} M*	*Total PPi/10^{-6} M* [b]	*RSD%*	*Recovery(%)*
1	6.0169	4.0	10.1534	2.1	103
2	5.6134	4.0	9.4221	1.8	95.2

[a] The results of a 1.8-fold diluted urine sample.

[b] The mean of six measurements.

GRAPHICAL ABSTRACT

Label-Free Fluorescence Polarization Detection of Pyrophosphate Based on 0D/1D Fast Transformation of CdTe Nanostructures

Jinyan Du, Li Ye, Meili Ding, Yuting Chen, Shujuan Zhuo, Changqing Zhu*

Key Laboratory of Functional Molecular Solids, Ministry of Education; Anhui Key Laboratory of Chemo-Biosensing, College of Chemistry and Materials Science, Anhui Normal University, Wuhu, 241000, PR China

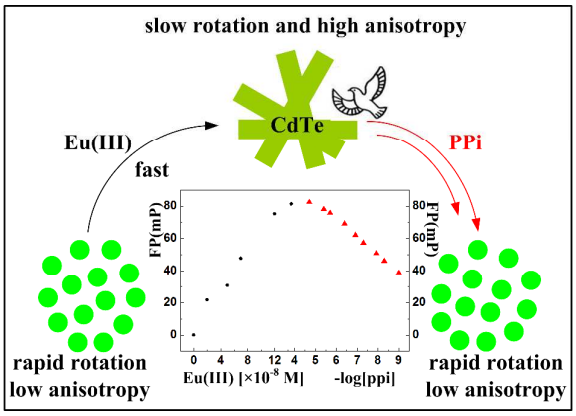

A novel and label-free fluorescence polarization method for detecting PPi was constructed based on 0D/1D fast rransformation of CdTe nanostructures

* Corresponding author.
E-mail address: zhucq@mail.ahnu.edu.cn